
Causally-Enhanced Reinforcement Policy Optimization

Xiangqi Wang¹, Yue Huang¹, Yujun Zhou¹, Xiaonan Luo¹, Kehan Guo¹ and Xiangliang Zhang¹

¹University of Notre Dame

xwang76, yhuang37, yzhou25, xluo6, kguo2, xzhang33@nd.edu

Large language models (LLMs) trained with reinforcement objectives often achieve superficially correct answers via shortcut strategies, pairing correct outputs with spurious or unfaithful reasoning and degrading under small causal perturbations. We introduce *Causally-Enhanced Policy Optimization* (CE-PO), a drop-in reward-shaping framework that augments policy optimization with a differentiable proxy for causal coherence along the generation pathway from prompt (Z) to rationale (X) to answer (Y). CE-PO estimates model-internal influence with Jacobian-based sensitivities, counterfactually hardens these signals to suppress nuisance cues, and fuses the resulting coherence score with task-accuracy feedback via a Minkowski (power-mean) combiner, exposing a single tunable between accuracy and coherence trade-off. The unified reward integrates with PPO/GRPO without architectural changes. Across reasoning benchmarks and causal stress tests, CE-PO reduces reward hacking and unfaithful chain-of-thought while improving robustness to correlation–causation flips and light counterfactual edits, all at near-parity accuracy. Experimental results across 4 datasets show that CE-PO improves accuracy over baselines by 5.49 % on average (up to 9.58 %), while improving robustness to correlation–causation flips and light counterfactual edits.

1. Introduction

Outcome-centric reinforcement training of large language models (LLMs)—whether via standard policy optimization or preference-based tuning [Christiano et al., 2017, Ouyang et al., 2022, Schulman et al., 2017, Shao et al., 2024] optimizes *what* answer is produced but places little pressure on *how* that answer is obtained [Sim et al., 2025]. As a result, models routinely learn to “game” reward signals (e.g., by exploiting length, format, or lexical overlap) and to pair correct answers with unfaithful or spurious reasoning traces [Wen et al., 2024, Arjovsky et al., 2020]. This failure mode is not merely theoretical: without intervention, we observe models can game both accuracy proxies and *gradient-based sensitivity* surrogates—e.g., by guessing final answer or maximizing output length as in section 3. This mismatch between scoring for outcomes and expecting coherent reasoning harms robustness, causing severe and threatening hallucination.

We argue that robust reasoning requires not only accurate outputs but also *causal coherence* along the generation pathway. By *coherence* we mean that (i) the prompt genuinely informs the rationale, (ii) the prompt along with rationale in turn genuinely informs the final answer, and (iii) small, causally relevant edits to the prompt or rationale induce correspondingly appropriate changes downstream, whereas irrelevant edits do not. Concretely, let $(Z \rightarrow X \rightarrow Y)$ denote the intended chain from prompt (Z), to rationale (X), to answer (Y) [Bao et al., 2024a]. If the model’s internal influence respects this order, chain-of-thought (CoT) [Wei et al., 2022] traces are more likely to be right for the right reasons [Ouyang et al., 2022, Shao et al., 2024] and to generalize under distribution shift. However, current reinforcement objectives offer no internal signal that rewards such coherence, as previous literature on causal reward in LLM typically focus on causally indifferent to external factors instead of reasoning coherence [Wang et al., 2025]. Related efforts to promote faithful reasoning typically

rely on external supervision or decoding-time control: rationale supervision and “right-for-the-right-reasons” regularizers require human explanations and usually target only input and generation; concept-bottleneck [Koh and Liang, 2017] and invariance/IRM approaches [Kamath et al., 2021] enforce intermediate structure but do not address generative $prompt \rightarrow rationale \rightarrow answer$ flows; CoT verification and constrained decoding act *post hoc* [Chi et al., 2025, Heimersheim et al., 2024] rather than shaping training. In contrast, we seek a *differentiable, annotation-free, training-time* signal that explicitly rewards influence coherence across $Z \rightarrow X \rightarrow Y$ and integrates into standard policy optimization.

Translating the above goal into a trainable signal raises three coupled issues. *Measurability*—existing faithfulness tools (saliency, raw input-gradient attributions) are fragile and can fail basic sanity checks or depend weakly on the learned model, limiting their usefulness as training signals [Adebayo et al., 2018]; gradient regularization that makes models “right for the right reasons” typically relies on human-provided rationales and targets only input \rightarrow output links in discriminative settings, not the generative $prompt \rightarrow rationale \rightarrow answer$ pathway [Ross et al., 2017], while causal-reasoning benchmarks show LLMs still conflate correlation and causation [Jin et al., 2024]. This motivates a *differentiable, model-internal* proxy for directed influence along $Z \rightarrow X$, $X \rightarrow Y$, and $Z \rightarrow Y$ that is compatible with policy-gradient optimization. *Robustness to spurious sensitivity*—naïve gradient signals are easily inflated by non-semantic factors (token frequency, position, format), encouraging shortcut learning [Geirhos et al., 2020] and *reward hacking* under outcome-only RL objectives [Amodei et al., 2016]; moreover, CoT can appear compelling yet remain unfaithful and brittle under small perturbations [Wei et al., 2022, Bao et al., 2024b, Chi et al., 2024]. Hence we require *counterfactual hardening* that explicitly breaks semantic links and filters out nuisance directions rather than trusting raw sensitivities. *Objective balance*—robustness-oriented methods (e.g., invariance penalties) often trade off in-distribution accuracy and can underperform ERM when mis-specified [Arjovsky et al., 2020, Rosenfeld et al., 2020, Kamath et al., 2021], whereas optimizing only task reward preserves shortcut exploitation [Amodei et al., 2016]. We therefore need a *tunable* mechanism to balance accuracy against coherence during optimization, avoiding both over-regularization and reward hacking.

Our approach. We introduce Causally-Enhanced Policy Optimization(CE-PO)¹, a drop-in reward-shaping scheme that adds a *Jacobian-based causal-coherence signal* to standard policy optimization and fuses it with task accuracy via a *Minkowski (power-mean) combiner*. Concretely, we compute model-internal Jacobian influence signals for the $prompt \rightarrow rationale$ and $rationale \rightarrow answer$ links; harden them with a simple counterfactual procedure (removing the resulting nuisance directions by reshuffling) to reduce sensitivity to superficial cues; normalize and aggregate into a single *coherence score*; and combine this score with accuracy using a power-mean with tunable weights/exponent, yielding a single reward that trades off coherence and accuracy. The unified reward is plugged into PPO/GRPO without architectural changes. In summary, our contributions are threefold:

- We propose a differentiable, model-internal *DCE-proxy* (influence–coherence) reward along $Z \rightarrow X \rightarrow Y$, coupled with *counterfactual residualization* (see subsection 2.1) to suppress shortcut sensitivities and *reward hacking*.
- We introduce a *Minkowski (power-mean) combiner* (detailed in subsection 2.2) that exposes a tunable trade-off between task accuracy and causal-coherence signals, serving as a drop-in objective for PPO/GRPO with efficient reward computation.
- CE-PO demonstrates consistent performance improvements, supported by comprehensive ablation analyses and competitive out-of-distribution generalization. In addition, our study highlights notable generation patterns and offers insights into model behavior.

¹Code implementation is available at: <https://github.com/XiangqiWang77/causalrl>

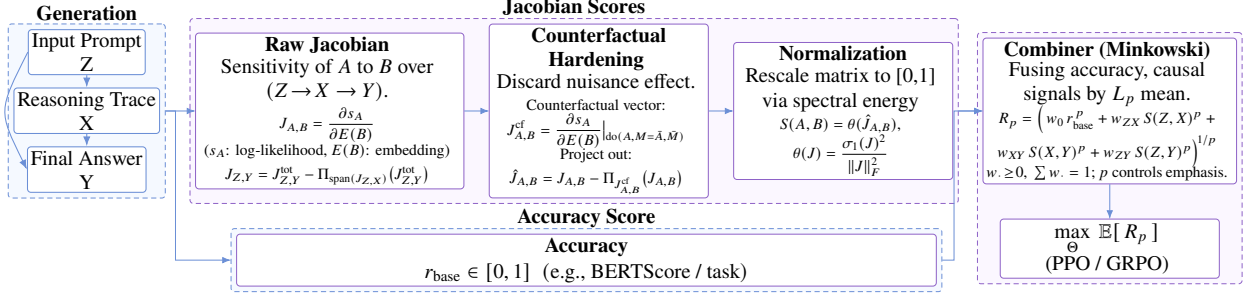


Figure 1: CE-PO pipeline (left \rightarrow right). *Generation*: $Z \rightarrow X \rightarrow Y$ (X/Y split by a special token; see Fig. 13). *Base Jacobians*: local sensitivities for $Z \rightarrow X$, $X \rightarrow Y$, $Z \rightarrow Y$. *Counterfactual hardening*: build source-side counterfactuals and project their subspace from the base signals to obtain hardened residuals. *Normalization*: use spectral energy to convert Jacobian matrix into $[0,1]$ scalar. *Fusion*: combine $S(A, B)$ signals with accuracy r_{base} via a Minkowski combiner; optimize the unified reward with PPO/GRPO.

2. Causal Enhanced Policy Optimization

Overview. In this section, we give implementation details of *CE-PO* and formalize it. Given a rollout with prompt Z , rationale X , and answer Y , as shown in Figure 1. The method unfolds in three steps that map one-to-one to the subsections below. (i) **Raw influence signals** : we compute *Base Jacobians*, i.e., local sensitivities of downstream span likelihoods with respect to upstream token embeddings, as differentiable, model-internal proxies for $Z \rightarrow X$, $X \rightarrow Y$, and for $Z \rightarrow Y$ removing mediator X . (ii) **Counterfactual hardening** : Deploying raw Jacobian scores as rewards risks *reward hacking*, where spurious factors (e.g., length) dominate the signal Figure 2. To suppress such shortcut and formatting sensitivities, we break semantic links (reshuffle/mismatch) and remove the induced nuisance directions from the raw signals. (iii) **Reward normalization and fusion** We normalize Jacobian responses into a stable scalar *coherence score* and then fuse it with task accuracy using a Minkowski (power-mean) combiner, yielding a unified reward that exposes a tunable accuracy–coherence trade-off and is optimized with PPO/GRPO. This section defines each component, provides complexity notes, and clarifies how they compose into the training loop.

2.1. Jacobian Signals, and Causally-Enhanced Reward

We consider a differentiable language model Θ and our goal is, as previously described, to improve the accuracy on Y (i.e., r_{base}) yet simultaneously to ensure the alignment of influence with this order: Z should shape X , and X, Z should shape Y . Our proposed method is illustrated in Figure 1, providing a causally grounded reward signal R_p by combining r_{base} and Jacobian-based scores measuring causal effects along $Z \rightarrow X \rightarrow Y$.

Base Jacobians. While Y -accuracy rewards *what* answer is produced, it does not constrain *how* the answer is obtained. To shape the reasoning pathway, we introduce a differentiable, model-internal *Direct Causal Effect (DCE) proxy* [Pearl, 2009, VanderWeele, 2011] for coherence along $Z \rightarrow X \rightarrow Y$: small and causal changes in upstream tokens should induce appropriate changes downstream. Concretely, let s_X and s_Y denote the log-likelihoods of the rationale span X and the answer span Y posterior to Z and Z, X as in Equation 1, and let $E(A) \in \mathbb{R}^{T_A \times d}$ be the token-embedding matrix for a text segment A (length T_A , hidden size d) and $a_{<t}$ denotes the prefix strictly before index t .

$$s_X = \sum_{t \in X} \log p_{\Theta}(x_t | Z, x_{<t}), \quad s_Y = \sum_{t \in Y} \log p_{\Theta}(y_t | Z, X, y_{<t}) \quad (1)$$

We measure the influence from A to the score of B by the *block Jacobian* $J_{AB} \triangleq \partial s_B / \partial E(A)$. For the intended chain $Z \rightarrow X \rightarrow Y$, the *Base Jacobians* (raw, unhardened sensitivities) are

$$J_{ZX} = \frac{\partial s_X}{\partial E(Z)} \in \mathbb{R}^{T_Z \times d}, \quad J_{XY} = \frac{\partial s_Y}{\partial E(X)} \in \mathbb{R}^{T_X \times d}, \quad J_{ZY}^{\text{total}} = \frac{\partial s_Y}{\partial E(Z)} \in \mathbb{R}^{T_Z \times d}. \quad (2)$$

In addition, to approximate the Direct Causal Effect (DCE) from Z to Y , we need to isolate X effect out of J_{ZY}^{total} . We remove the mediated path via projection: forming a *via- X* template from J_{ZX} ($Z \rightarrow X$) and the principal direction of J_{XY} ($X \rightarrow Y$), then subtracting its projection from the total effect to obtain the direct effect:

$$J_{ZY} = J_{ZY}^{\text{total}} - \Pi_{J_{ZX} \odot \bar{u}} \left(J_{ZY}^{\text{total}} \right), \quad (3)$$

where $\bar{u} = \frac{1}{T_X} \sum_{t \in X} \frac{J_{XY}[t,:]}{\|J_{XY}[t,:]\|_2}$, and $\Pi_A(B) = \frac{\langle B, A \rangle_F}{\langle A, A \rangle_F} A$, with $\langle B, A \rangle_F$ indicating the Frobenius inner product between A and B , and \odot be Hadamard product.

We use the Jacobian as a local, direct causal effect *proxy*: for any upstream–downstream pair $(A, B) \in \{(Z, X), (X, Y), (Z, Y)\}$, with mediators held at their observed values, $J_{AB} = \partial s_B / \partial E(A)$ quantifies how an infinitesimal perturbation to A ’s embeddings shifts the downstream log-likelihood s_B —i.e., which directions in A immediately move B , and by how much. Crucially, J_{AB} is not equal to a causal DCE in the mediation sense; it is the *first-order Taylor approximation* around the observed point [Pearl, 2001]. They are already informative enough and avoid the cost and instability of higher-order (Hessian/influence-function) estimators in deep/LLM settings [Pearlmutter, 1994, Martens, 2010, Koh and Liang, 2017, Li et al., 2024].

We use J_{AB} to serve as the starting point for our *coherence* signal. In the next subsections we apply *counterfactual hardening* to remove nuisance directions and then normalize/aggregate the residual influence into a scalar coherence score that is fused with task accuracy.

Counterfactual-hardened Jacobian score. Jacobian-based rewards, when computed directly on the base input, may conflate causal content with nuisance factors such as style, formatting and token-frequency statistics. As a result, innocuous paraphrases or vacuous elongation can inflate the gradient norm and concentrate its top singular direction, enabling *length-driven reward hacking* up to the token limit [Gao et al., 2023, Rafailov et al., 2024]. Empirically, as shown in Figure 2 (blue), the length hacking existing in non-counterfactual Jacobian rewards (Non-CF-GRPO conflates).

To suppress shortcut-driven sensitivities in the *Base Jacobians*, we harden them with pair-specific counterfactuals. For each link $(A, B) \in \mathcal{L} := \{(Z, X), (X, Y), (Z, Y)\}$, let $M(A, B)$ denote mediators on $A \rightarrow B$ paths (empty except $M(Z, Y) = \{X\}$). We break the semantic alignment between A (and M) and B by permuting the tokens of A (and of M when present), yielding (\bar{A}, \bar{M}) that preserves surface statistics (length/frequency) while being approximately independent of B . Let s_B be the log-likelihood of span B and $E(A) \in \mathbb{R}^{T_A \times d}$ the embedding matrix of A . We compute the *counterfactual Jacobian*

$$J_{AB}^{\text{cf}} = \left. \frac{\partial s_B}{\partial E(A)} \right|_{(A, M) \mapsto (\bar{A}, \bar{M})}. \quad (4)$$

We construct K *source-side* counterfactuals and calculate their Jacobians by Equation 4, which are then averaged to have \bar{J}_{AB}^{cf} (we set $K=4$, larger values generally improve results but incur higher computational cost).

Then, we extract the principal counterfactual subspace via the top- k left singular vectors U_{AB} of J_{AB}^{cf} , define the projector $\Pi_{AB}(J) = U_{AB} U_{AB}^\top J$, following [Ravfogel et al., 2020]. Taking the J_{AB} in Equation 2 and Equation 3, we obtain the deconfounded (direct) block by removing these directions:

$$\hat{J}_{AB} = J_{AB} - \Pi_{AB}(J_{AB}). \quad (5)$$

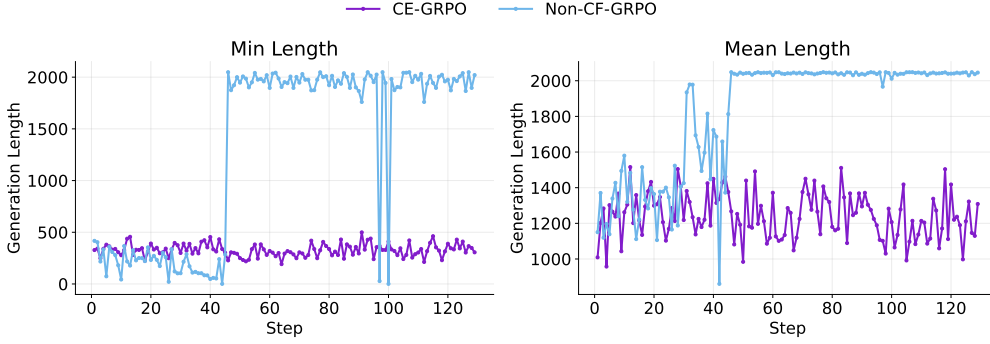


Figure 2: Training trajectories comparison: **Non-CF-GRPO** (GRPO with non-CF award) vs **CE-GRPO** (GRPO with our CE award) on Qwen-3-4B-Thinking with `max_tokens=2048`, in terms of minimum (left) and mean (right) generation length. Non-CF-GRPO curves plateau as generations approach the token limit, indicating length-driven reward hacking, while CE-GRPO doesn’t.

Permuted signals expose a spurious nuisance subspace; projecting it out yields a deconfounded, causally aligned signal that resists surface correlations and reward hacking [Ravfogel et al., 2020].

As shown in Figure 2 (purple), the Non-CF-GRPO baseline drives the mean generation length to the token cap, revealing a length-based reward-hacking loop. With our counterfactual reshuffling and projection (CE-GRPO), the curve stays well below the cap and does not plateau, while reward improves. The mechanism is simple: source-side counterfactuals preserve surface statistics (length/frequency) while scrambling semantics [Ravfogel et al., 2020], so the counterfactual Jacobian spans a nuisance subspace; orthogonally projecting the base Jacobian off this subspace—akin to Neyman orthogonalization [Oprescu et al., 2019]—decouples the reward from length/format sensitivities and correlations [Chernozhukov et al., 2018]. For the $Z \rightarrow Y$ link, we additionally subtract the via- X component before projection (a first-order direct-effect correction), further reducing spurious incentives.

Reward normalization and fusion Finally, we *scalarize* the block to a score via the scale-free spectral energy share $S(A, B) = \phi(\hat{J}_{AB})$, where $\phi(J) = \sigma_1(J)^2 / \|J\|_F^2 \in [0, 1]$ to squeeze and standardize the process [Vershynin, 2018]. Concretely,

$$S(Z, X) = \phi(\hat{J}_{ZX}), \quad S(X, Y) = \phi(\hat{J}_{XY}), \quad S(Z, Y) = \phi(\hat{J}_{ZY}). \quad (6)$$

Let $r_{\text{base}} \in [0, 1]$ be a task accuracy score on Y (e.g., semantic correctness, measured by BERTScore [Zhang et al., 2019] in our setting). We define the new causally grounded reward by integrating accuracy and the three counterfactual-enhanced signals via a weighted power mean (Minkowski combiner) [Bullen, 2013],

$$R_p = \left(w_0 r_{\text{base}}^p + w_1 S(Z, X)^p + w_2 S(X, Y)^p + w_3 S(Z, Y)^p \right)^{1/p}, \quad (7)$$

with $p \in \mathbb{R}$, weights $w_i \geq 0$, and $\sum_{i=0}^3 w_i = 1$. As $p \rightarrow 0$, R_p approaches a weighted geometric mean (minimal optimization); larger p emphasizes the largest channel, which respectively matches deconfounded Jacobian causal scores and BERTScore as in subsection 2.2. Using this R_p in any common policy-gradient training of LLM (e.g., PPO, GRPO), the goal is to maximize $\mathbb{E}[R_p]$.

Note of r_{base} : We set r_{base} by BERTScore (i.e., the cosine similarity between Y and ground truth in BERT embedding space), as it is a continuous measure between 0 and 1 for accuracy, aligning with the scale of the causal term. In contrast, 0/1 judgments are often sensitive to judging prompts and are less compatible; mixing such binary signals with the causal term can induce oscillatory updates. Ablation studies on replacing BERTScore with 0/1 rewards are provided in Figure 3. In addition, we also provide TRPO-form [Schulman et al., 2015] lower bound for CE-PO with details in Appendix B and the discussion for training efficiency can be found in Appendix C.

Training objective Let $R_p(Z, X, Y) \in [0, 1]$ denote the unified reward from Eq. (7). We treat R_p as a scalar terminal reward for each rollout (Z, X, Y) : $r_T = R_p$, $r_t = 0$ for $t < T$, and **do not backpropagate through R_p** (standard policy-gradient; the Jacobian signals are used only to compute R_p).

CE-PPO. With behavior policy π_{old} , importance ratio $w_t(\theta) = \pi_\theta(a_t|s_t)/\pi_{\text{old}}(a_t|s_t)$, and GAE advantages \hat{A}_t computed from the sparse reward, the clipped objective is

$$\mathcal{J}_{\text{CE-PPO}}(\theta) = \mathbb{E} \left[\min(w_t(\theta)\hat{A}_t, \text{clip}(w_t(\theta), 1-\epsilon, 1+\epsilon)\hat{A}_t) - \beta \text{KL}(\pi_\theta \parallel \pi_{\text{ref}}) \right]. \quad (8)$$

We optionally standardize R_p per batch to stabilize advantages.

CE-GRPO. For each prompt we sample K candidates, compute $R_{p,k}$, and form group-relative advantages $\tilde{A}_k = (R_{p,k} - \mu_{\text{grp}})/(\sigma_{\text{grp}} + \epsilon)$, with $\mu_{\text{grp}}, \sigma_{\text{grp}}$ the group mean/std. The GRPO-style objective is

$$\mathcal{J}_{\text{CE-GRPO}}(\theta) = \mathbb{E} \left[\frac{1}{K} \sum_{k=1}^K \min(w_k(\theta)\tilde{A}_k, \text{clip}(w_k(\theta), 1-\epsilon, 1+\epsilon)\tilde{A}_k) - \beta \text{KL}(\pi_\theta \parallel \pi_{\text{ref}}) \right]. \quad (9)$$

2.2. Reward Signals Trade-off

Our RL objective (maximizing $\mathbb{E}[R_p]$) blends two signals, semantic accuracy (e.g., BERTScore) and causal coherence (counterfactual-enhanced Jacobian). These signals misalign at times, mirroring RLHF’s trade-off between surface correctness and shortcut avoidance [Kalai et al., 2025, Lightman et al., 2023]. By defining R_p via the Minkowski norm, we enable a dynamically tunable balance between the two signals.

Figure 3 illustrates how the Minkowski p -norm interpolation provides a smooth mechanism to mediate the trade-off between semantic accuracy and causal coherence. As $p \rightarrow +\infty$, the reward collapses to the larger signal, typically BERTScore, which is unprojected and numerically higher. This drives accuracy-focused optimization (as observed in all models). Conversely, as $p \rightarrow -\infty$, the reward collapses to the smaller signal (e.g., when $p = 0$ the interpolation equals geometric mean), which is usually the counterfactual Jacobian, lowered by residualization. This, in turn, emphasizes causal coherence. This multi-objective behavior parallels prior work on balancing conflicting RL rewards [Won et al., 2019, Roijers et al., 2013]. To illustrate how CE-PO combine both signals can thus enhance LLM reasoning capability to be both causally capable yet not template-following, we provide an LLM generation example in Figure D.

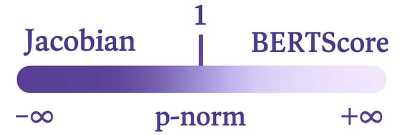


Figure 3: Tunable balance enabled by Minkowski p -norm interpolation in R_p .

3. Experiments

In this section, we show performance of CE-PO on top of PPO and GRPO (noted as **CE-PPO** or **CE-GRPO**) against simple baselines, using BERTScore as the reward (denoted as PPO-BERTScore or GRPO-BERTScore) and vanilla LLMs, across representative LLMs and standard evaluation datasets.

Experiment Setting. Training is performed on a single node with four A100 or H100 GPUs. Unless stated otherwise, we use a rollout group size of 6 per prompt, KL penalty of $\lambda_{\text{KL}} = 0.001$ to stabilize optimization, and cap decoder outputs at 2048 tokens and input within 512 tokens. In determining R_p , extensive experiments indicate that a good configuration could be $p = 0.2$ and BERTScore, Jacobian scores weights, respectively, as $(w_0, w_1, w_2, w_3) = (0.7, 0.1, 0.1, 0.1)$, which is set as default for comparison unless otherwise specified in ablation studies. We set learning rate of 2×10^{-6} ,

batch size 32, and training for 10 epochs with temperature 0.6. Validation interval is set as 10 and checkpoints are saved per 100 steps. Experiments are based on Verl [Sheng et al., 2024] framework with mild modification for separate thread for reward calculation, and we also set warm-up step = 10 for critic.

To avoid random guesses, all models are prompted to generate CoT reasoning [Wei et al., 2022]. Evaluation is reported as accuracy, and the response correctness is determined via an LLM-as-Judge protocol [Zheng et al., 2023] using GPT-4o-mini (see prompt in Figure 14, which is designed to distinguish guess or contradictions especially for multi-choice questions).

We evaluate both standard instruction-tuned LLMs and “thinking” variants that emit explicit intermediate reasoning and instruction following. Although compute constraints preclude experiments on 70B-scale models, our evaluation covers compact to mid-sized systems that are widely used in research: Llama-3-8B-Instruct, Llama-3.2-3B-Instruct, Phi-3.5-mini-Instruct, Qwen3-4B-Thinking, and Qwen3-1.7B-Thinking [Meta AI, 2024b,a, Microsoft, 2025, Qwen Team, 2025b,a].²

Training and Validation Dataset. We train and tune on four reasoning-heavy sets: *BBEHCausal*, the causal reasoning split from BIG-Bench Extra Hard dataset, including counterfactual deduction or cause inference questions; [Google DeepMind, 2025]); *CaseHOLD*, tasks centering on multiple-choice legal holdings given case citation context [CaseHOLD, 2022]; *MATHHARD*, the level-5 subset targeting multi-step mathematical reasoning with multiple-choice questions [Hendrycks et al., 2021]; and *IfQA*, an open-domain QA under counterfactual *if*-clause presuppositions requiring hypothetical reasoning [Yu et al., 2023]. Note that all datasets are formatted as question answer pairs, examples of them are presented respectively in Table 4 and Table 5.

Testing Dataset. For same-field evaluation, we use *BBEHMATH* (challenging multistep arithmetic), where we filter shorter and more trivial questions and normalize alphabetic numerals to digits with unfolded calculation for comparability on this dataset [Google DeepMind, 2025]. We further assess generalization with *CLadder*, covering association/intervention/counterfactual queries [Causal-NLP, 2023], *LegalBench* (case-understanding split) [Guha et al., 2023] analyzing the cause or reason of legal case, and *LogiQA*, a multiple-choice dataset emphasizing deductive logical reasoning sourcing from officer entrance exams [lucasmccabe, 2021].

Main Experiment Results. Under the training and validation dataset split detailed above, Figure 4 shows CE-PPO delivering smooth, near-monotonic validation gains across five backbones and four validation sets: rapid early improvement followed by mild saturation, which is indicative of stable and standard RL optimization plot rather than overfitting. In Table 1, across all five backbones, both causal variants outperform their non-causal baselines: CE-PPO/CE-GRPO improve the best non-CE baseline by 2.3 to 9.58 points. Comparing CE-GRPO with the vanilla baseline, we observe gains of 5.8–6.0 points on Llama-3-8B and Llama-3.2-3B; the largest improvement appears on Qwen-3-1.7B-Thinking (≈ 10 points), whereas Phi-3.5-mini-Instruct shows the most marginal uplift. These patterns suggest that architectural and scale differences modulate the benefits of CE-GRPO. CE-GRPO is *not* uniformly stronger than CE-PPO, while slightly higher on Qwen-1.7B/4B, Phi-3.5-mini, and Llama-3-8B, it lags behind CE-PPO on Llama-3.2-3B, indicating complementary strengths rather than strict dominance.

Out of Distribution(OOD) Evaluation. Trained exclusively on causal- and math-reasoning corpora, our CE-PO models are stress-tested for OOD generalization on TruthfulQA [Lin et al., 2021] (misconception resistant factuality), CodeMMLU [Manh et al., 2024] (programming knowledge), and SuperGPQA [Du et al., 2025] (expert level STEM QA), evaluating 200 uniformly random samples from

²Note that all experiments use Instruct or Thinking models, as our outputs must be cleanly formatted into X and Y , which base models struggle to separate. Since Instruct models are typically harder to improve with RL, the observed gains further highlight the effectiveness of CE-PO.

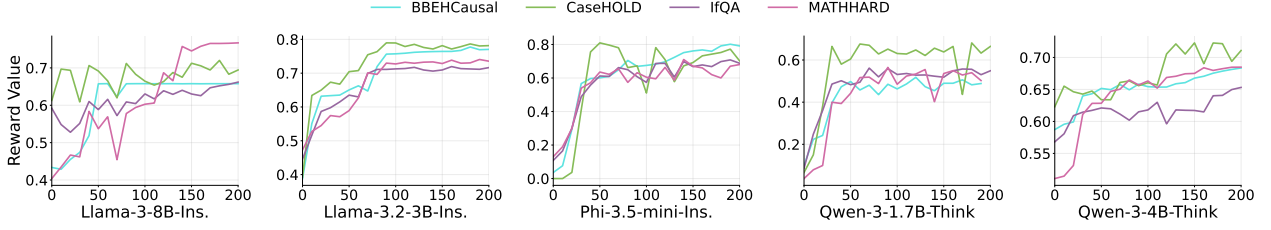


Figure 4: Reward curves of CE-PPO training on validation datasets across five models.

Table 1: Main results across models, RL methods, and datasets. We report LLM-as-Judge accuracy (%) under different RL variants: vanilla model, standard PPO/GRPO with BERTScore reward, and causal-enhanced (CE-PPO/CE-GRPO). We repeatedly generate 4 times of each trained model, and thus report mean and deviation below.

Model	RL Method	Dataset (%)				Average
		BBEHMATH	CLadder	LegalBench	LogiQA	
Qwen-3-1.7B-Thinking	Vanilla	1.36 ± 1.96	34.77 ± 0.68	57.80 ± 2.59	50.00 ± 0.45	35.98
	PPO-BERTScore	5.91 ± 0.00	37.27 ± 0.91	58.26 ± 1.95	52.50 ± 0.00	38.48
	GRPO-BERTScore	3.64 ± 1.29	35.00 ± 0.52	60.67 ± 0.94	57.04 ± 0.68	39.09
	CE-PPO	10.45 ± 0.52	49.32 ± 0.68	60.67 ± 1.05	58.05 ± 1.14	44.62
	CE-GRPO	10.00 ± 1.29	44.77 ± 0.00	70.64 ± 0.00	56.82 ± 0.45	45.56
Qwen-3-4B-Thinking	Vanilla	6.82 ± 0.45	42.95 ± 0.91	74.77 ± 1.95	80.45 ± 0.68	51.25
	PPO-BERTScore	5.00 ± 1.05	45.00 ± 0.00	73.64 ± 0.47	80.00 ± 0.45	50.91
	GRPO-BERTScore	6.82 ± 0.45	40.68 ± 0.68	76.61 ± 0.65	83.86 ± 0.91	51.99
	CE-PPO	9.55 ± 0.52	45.45 ± 0.68	79.34 ± 1.05	79.77 ± 0.91	53.53
	CE-GRPO	7.27 ± 0.00	49.09 ± 0.64	76.90 ± 0.00	84.09 ± 0.45	54.34
Phi-3.5-mini-Ins.	Vanilla	6.13 ± 0.52	40.23 ± 0.68	68.35 ± 1.95	54.09 ± 0.45	42.20
	PPO-BERTScore	6.59 ± 0.00	43.40 ± 0.87	66.97 ± 0.00	54.77 ± 0.00	42.93
	GRPO-BERTScore	5.45 ± 0.87	41.59 ± 0.64	68.81 ± 1.30	52.73 ± 0.45	42.15
	CE-PPO	8.41 ± 0.00	42.95 ± 0.91	70.18 ± 1.95	55.90 ± 0.68	44.36
	CE-GRPO	6.81 ± 0.64	45.45 ± 0.45	70.18 ± 0.65	57.95 ± 0.00	45.10
Llama-3.2-3B-Ins.	Vanilla	3.63 ± 0.91	30.00 ± 0.68	45.41 ± 0.47	41.59 ± 0.45	30.16
	PPO-BERTScore	6.59 ± 0.68	33.63 ± 0.64	45.87 ± 0.00	38.41 ± 0.45	31.12
	GRPO-BERTScore	6.50 ± 0.45	31.36 ± 0.91	42.73 ± 2.57	44.09 ± 0.00	31.17
	CE-PPO	10.67 ± 1.14	43.64 ± 0.68	55.05 ± 1.30	48.18 ± 0.91	39.38
	CE-GRPO	7.95 ± 0.91	35.23 ± 0.00	54.13 ± 2.59	47.27 ± 0.45	36.15
Llama-3-8B-Ins.	Vanilla	7.05 ± 0.45	39.54 ± 0.91	61.93 ± 1.95	65.68 ± 0.64	43.55
	PPO-BERTScore	5.27 ± 0.64	37.95 ± 0.00	61.93 ± 0.00	60.91 ± 0.45	41.52
	GRPO-BERTScore	10.91 ± 1.14	39.09 ± 0.91	57.80 ± 0.00	67.50 ± 0.00	43.83
	CE-PPO	14.86 ± 1.59	44.77 ± 0.45	67.35 ± 0.79	68.40 ± 0.91	48.84
	CE-GRPO	13.64 ± 0.91	45.00 ± 0.64	66.97 ± 0.00	71.82 ± 0.45	49.36

each benchmark. As shown in Figure 5, they deliver consistent—but task-dependent improvements over baselines: effects are strongest on structure-heavy code reasoning, moderate on STEM-oriented SuperGPQA, and smaller yet steady on TruthfulQA, suggesting that causal regularization chiefly benefits multi-step reasoning while preserving overall robustness.

Ablation Studies. We test CE-PO’s composite objective under a fixed setup (Llama-3-8B-Instruct, GRPO, max_tokens=2048; datasets: BBEHMath, CLadder, LegalBench, LogiQA). The base reward is r_{base} (BERTScore); coherence uses hardened link scores $S(Z, X)$, $S(X, Y)$, $S(Z, Y)$. We ablate the Minkowski exponent p and weights w , drop individual links, add Gaussian noise to r_{base} , and swap BERTScore for an LLM-as-Judge. Ablation results in Table 2 yield:

Insight 1: Reward hacking would emerge once we remove any of $S(Z, X)$, $S(Z, Y)$ and $S(X, Y)$. Models under such flawed RL can’t even excel the original models as observed in row 5 to 7 in Table 2.

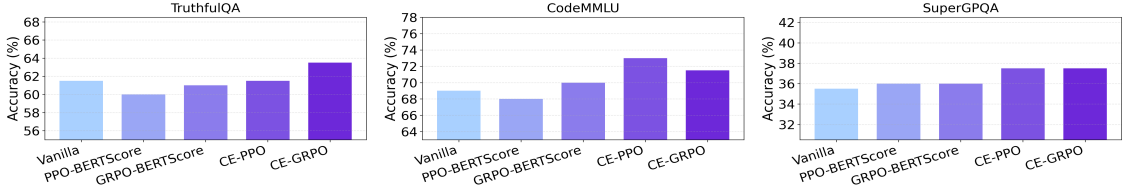


Figure 5: Qwen-3-4B-Thinking accuracy in OOD evaluation scenarios.

Table 2: Ablation Studies on Llama-3-8B-Ins.

Ablation	BEBHMATH	CLadder	LegalBench	LogiQA	Average
$p = 10$	6.36	39.09	56.90	67.27	42.91
$p = -2$	12.73	43.63	65.52	70.00	47.97
$p = 1$	10.00	50.00	60.34	64.55	46.22
$w=[0, 1/3, 1/3, 1/3]$	10.91	44.54	61.93	68.18	46.89
$w=[4/5, 1/10, 1/10, 0]$	5.45	23.63	40.37	41.82	27.82
$w=[4/5, 1/10, 0, 1/10]$	3.63	30.00	45.87	49.09	32.15
$w=[4/5, 0, 1/10, 1/10]$	5.45	31.82	43.12	40.90	30.32
$w=[1/2, 1/6, 1/6, 1/6]$	8.18	41.82	67.24	66.36	45.90
Perturbed Reward	7.27	40.00	65.52	69.09	45.97
Judge Reward (binary)	6.36	39.09	60.34	66.36	43.04
CE-GRPO	13.64	47.27	66.97	72.73	50.65

The likely cause is an incomplete constraint, i.e., the causal loop $Z \rightarrow X \rightarrow Y$ is not closed, so the optimization ceases to be strictly benign. With a detailed supporting plot provided in Figure 11 of the reward signal and generation length, we can observe that initial removal breaks the prior balance (reward dips), and subsequent updates discover a length shortcut (length conflating).

Insight 2: By selecting different p values, we can observe the performances of p as 10 identical to BERTScore only and p as -2 to Jacobian scores only (i.e. w as $[0, 1/3, 1/3, 1/3]$). The same case of p as 1, which reveals that tuning p can dynamically tune the optimization objective.

Insight 3: Under a perturbed reward (Gaussian noise $\sigma=0.05$), the model maintains satisfactory performance, indicating robustness of the training design. Using GPT - 4o - mini as an LLM-as-Judge (vs. BERTScore) yields performance similar to the original model, revealing what’s prescribed in the Note of r_{base} in subsection 2.1.

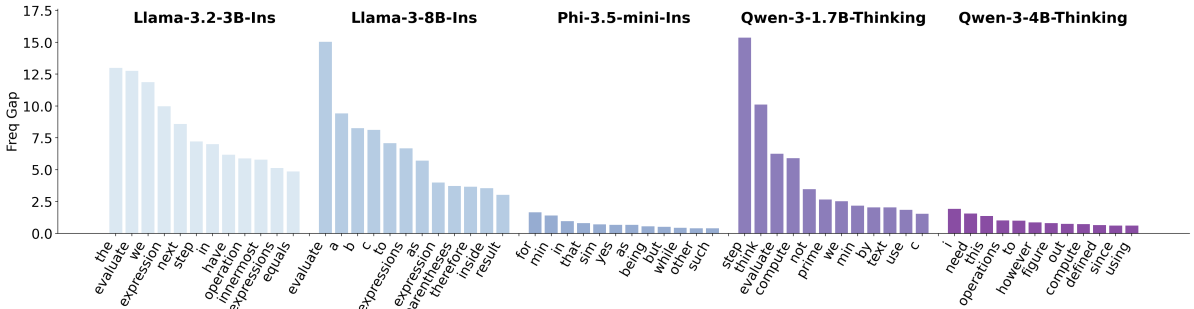


Figure 6: Frequency gap of generation per word where CE-GRPO exceeds BERTScore and Vanilla LLM (Top-12 per model).

Generation Pattern Analysis. Figure 6 shows that CE-GRPO does not induce uniform gains across all tokens but selectively amplifies reasoning or causal related words, suggesting that causal regularization guides the model toward tokens central to stepwise inference rather than surface templates. Complementarily, Figure 9 reveals the structural relation between metrics: $S(Z, X)$ is nearly independent of $S(X, Y)$ and $S(Z, Y)$, while the latter two are moderately correlated. This indicates that

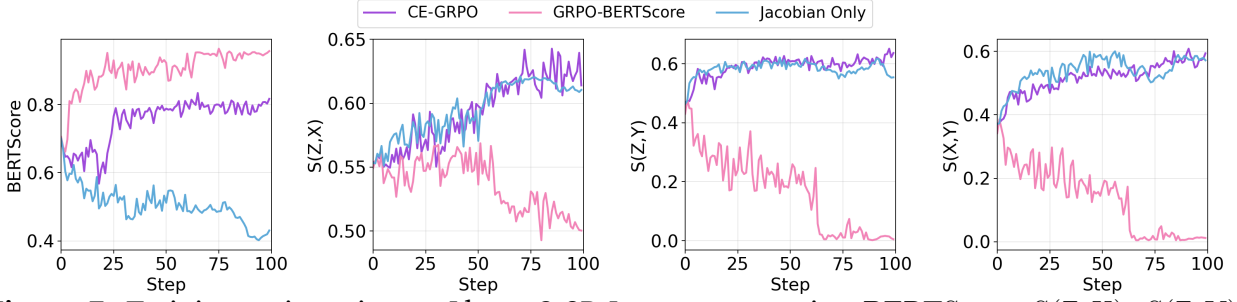


Figure 7: Training trajectories on Llama-3-8B-Instruct, reporting BERTScore, $S(Z, X)$, $S(Z, Y)$, $S(X, Y)$ (left to right). Comparison is made between CE-GRPO and optimization with only causal signal (Jacobian) or accuracy signal (BERTScore), supporting the claim of reward signal balance in subsection 2.2.

“evidence infusion” and “answer stability” provide orthogonal yet complementary signals. Their joint use, as in CE-GRPO, therefore supports coherence across the full $Z \rightarrow X \rightarrow Y$ pathway, rather than relying on any single proxy.

Turning to sequence-level behavior, Figure 8 reports the response lengths of CE-GRPO, GRPO-BERTScore, and the vanilla model on the training sets. The means are closely matched, indicating our optimization is largely *length-indifferent*. CE-GRPO achieves better task performance without increasing the token budget beyond the baseline, suggesting the efficiency of CE-GRPO.

Finally, the training reward trajectories in Figure 7 highlight three regimes: BERTScore-only optimization inflates BERTScore only while collapsing causal channels, Jacobian-only boosts sensitivities but remains unstable and harms task accuracy. This finding echoes prior work showing that proxy metric optimization (e.g., ROUGE) misaligns with human preferences [Stiennon et al., 2020], while self-rewarded training inflates output length, underscoring the tension between verifiable rewards and reward-gaming behaviors [Yuan et al., 2025]. CE-GRPO achieves smooth improvements across $S(Z, X)$, $S(X, Y)$, and $S(Z, Y)$ while keeping BERTScore competitive. This pattern underscores CE-GRPO’s ability to sustain the causal chain from prompt to reasoning to answer, offering a practical safeguard against shortcut learning.

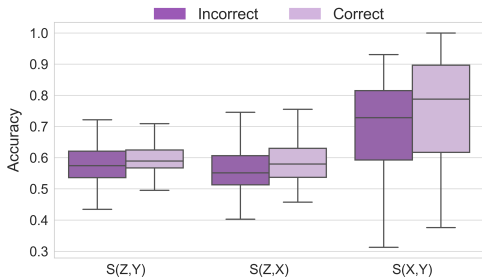


Figure 10: Boxplots of $S(Z, X)$, $S(Z, Y)$, and $S(X, Y)$ for LLM-as-Judge accuracy regarding their causal trajectory.

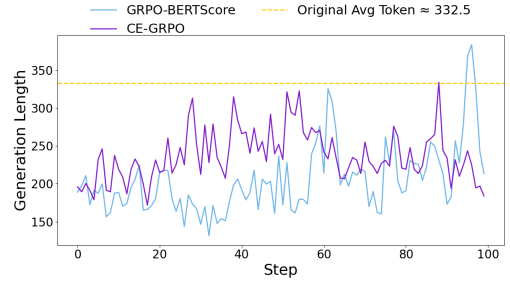


Figure 8: Response length comparison on Llama-3-8B-Ins

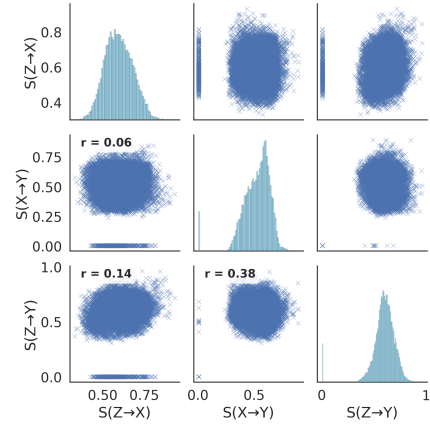


Figure 9: Pairwise scatter matrix of causal metrics on Qwen-3-4B-Thinking.

Jacobian Signals and Accuracy Figure 10 shows the distributions of Jacobian-based scores for samples annotated by correctness with LLM-as-Judge with strict judging criteria provided in Figure 14 conducted by GPT-4o. Annotations were collected on 1000 samples generated by Llama-3-8B-Ins. In total, 371 cases were labeled as consistent and 629 as inconsistent. To assess differences between the two groups, we conducted t-test with results reported in Table 3. We evaluate whether higher $S(A, B)$ scores align with factual correctness, as validity of these

causal signals requires separation under strict accuracy criteria. As in Table 3, all three metrics show significantly higher means for the correct group ($p < 0.01$), confirming that $S(A, B)$ faithfully tracks reasoning–answer validity beyond surface outputs, and by statistically aligns with cognitive accuracy.

4. Conclusion

We propose counterfactual-enhanced policy optimization that couples task accuracy with continuous causal signals, yielding smoother training and consistent gains across models and datasets, especially on Thinking backbones. The approach is a drop-in for PPO/GRPO and reduces reward-hacking behaviors, improving stability during training and robustness at convergence. Future work based on CE-PO could possible work on scale interventions and automate the accuracy–causality balance; CE-PO opens new optimization avenues by incorporating richer causal signals (e.g., Hessian-based beyond simple Jacobian) and enabling adaptive schemes that tune this trade-off on the fly.

References

- Julius Adebayo, Justin Gilmer, Michael Muelly, Ian Goodfellow, Moritz Hardt, and Been Kim. Sanity checks for saliency maps. *Advances in neural information processing systems*, 31, 2018.
- Dario Amodei, Chris Olah, Jacob Steinhardt, Paul Christiano, John Schulman, and Dan Mané. Concrete problems in ai safety. *arXiv preprint arXiv:1606.06565*, 2016.
- Martin Arjovsky, Léon Bottou, Ishaan Gulrajani, and David Lopez-Paz. Invariant risk minimization. In *International Conference on Learning Representations (ICLR)*, 2020.
- Fan Bao et al. Non-causal reasoners in large language models. *arXiv preprint arXiv:2407.01489*, 2024a.
- Guangsheng Bao, Hongbo Zhang, Linyi Yang, Cunxiang Wang, and Yue Zhang. Llms with chain-of-thought are non-causal reasoners. *arXiv preprint arXiv:2402.16048*, 2024b.
- Atilim Gunes Baydin, Barak A. Pearlmutter, Alexey A. Radul, and Jeffrey Mark Siskind. Automatic differentiation in machine learning: A survey. *Journal of Machine Learning Research*, 18(153):1–43, 2018. URL <https://jmlr.org/papers/v18/17-468.html>.
- Peter S Bullen. *Handbook of means and their inequalities*, volume 560. Springer Science & Business Media, 2013.
- CaseHOLD. Casehold. Hugging Face dataset, 2022. URL <https://huggingface.co/datasets/casehold/casehold>.
- Causal-NLP. Cladder. Hugging Face dataset, 2023. URL <https://huggingface.co/datasets/causal-nlp/CLadder>.
- Victor Chernozhukov, Denis Chetverikov, Mert Demirer, Esther Duflo, Christian Hansen, Whitney Newey, and James Robins. Double/debiased machine learning for treatment and structural parameters, 2018.
- Haoang Chi, He Li, Wenjing Yang, Feng Liu, Long Lan, Xiaoguang Ren, Tongliang Liu, and Bo Han. Unveiling causal reasoning in large language models: Reality or mirage? In *Advances in Neural Information Processing Systems (NeurIPS)*, 2024.
- Zhenyu Chi et al. Unveiling causal reasoning in large language models via g²-reasoner. *arXiv preprint arXiv:2503.13846*, 2025.
- Paul F. Christiano, Jan Leike, Tom B. Brown, Miljan Martic, Shane Legg, and Dario Amodei. Deep reinforcement learning from human preferences. In *Advances in Neural Information Processing Systems (NeurIPS)*, 2017.
- Xinrun Du, Yifan Yao, Kaijing Ma, Bingli Wang, Tianyu Zheng, King Zhu, Minghao Liu, Yiming Liang, Xiaolong Jin, Zhenlin Wei, et al. Supergpqa: Scaling llm evaluation across 285 graduate disciplines. *arXiv preprint arXiv:2502.14739*, 2025.
- Tom Everitt, Victoria Krakovna, Laurent Orseau, Marcus Hutter, and Shane Legg. Reinforcement learning with a corrupted reward channel. *arXiv preprint arXiv:1705.08417*, 2017.
- Leo Gao, John Schulman, and Jacob Hilton. Scaling laws for reward model overoptimization. In *Proceedings of the 40th International Conference on Machine Learning, ICML*. PMLR, 2023. URL <https://proceedings.mlr.press/v202/gao23h/gao23h.pdf>.

- Robert Geirhos, Jörn-Henrik Jacobsen, Claudio Michaelis, Richard Zemel, Wieland Brendel, Matthias Bethge, and Felix A Wichmann. Shortcut learning in deep neural networks. *Nature Machine Intelligence*, 2(11):665–673, 2020.
- Gene H. Golub and Charles F. Van Loan. *Matrix Computations*. Johns Hopkins University Press, 4 edition, 2013. URL <https://math.ecnu.edu.cn/~jypan/Teaching/books/2013%20Matrix%20Computations%204th.pdf>.
- Google DeepMind. Big-bench extra hard (bbeh). GitHub repository, 2025. URL <https://github.com/google-deepmind/bbeh>.
- Neel Guha, Julian Nyarko, Daniel E. Ho, Christopher Ré, Adam Chilton, Aditya Narayana, Alex Chohlas-Wood, Austin Peters, Brandon Waldon, Daniel N. Rockmore, Diego Zambrano, Dmitry Talisman, Enam Hoque, Faiz Surani, Frank Fagan, Galit Sarfaty, Gregory M. Dickinson, Haggai Porat, Jason Hegland, Jessica Wu, Joe Nudell, Joel Niklaus, John Nay, Jonathan H. Choi, Kevin Tobia, Margaret Hagan, Megan Ma, Michael Livermore, Nikon Rasumov-Rahe, Nils Holzenberger, Noam Kolt, Peter Henderson, Sean Rehaag, Sharad Goel, Shang Gao, Spencer Williams, Sunny Gandhi, Tom Zur, Varun Iyer, and Zehua Li. Legalbench: A collaboratively built benchmark for measuring legal reasoning in large language models, 2023.
- Sören Heimersheim et al. How to use and interpret activation patching. *arXiv preprint arXiv:2405.05964*, 2024.
- Dan Hendrycks, Collin Burns, Saurav Kadavath, Akul Arora, Steven Basart, Eric Tang, Dawn Song, and Jacob Steinhardt. Measuring mathematical problem solving with the math dataset. *arXiv preprint arXiv:2103.03874*, 2021.
- Zhijing Jin, Jiarui Liu, Zhiheng Lyu, Spencer Poff, Mrinmaya Sachan, Rada Mihalcea, Mona T. Diab, and Bernhard Schölkopf. Can large language models infer causation from correlation? In *International Conference on Learning Representations (ICLR)*, 2024.
- Adam Tauman Kalai, Ofir Nachum, Santosh S. Vempala, and Edwin Zhang. Why language models hallucinate, 2025. URL <https://arxiv.org/abs/2509.04664>.
- Pritish Kamath, Akilesh Tangella, Danica Sutherland, and Nathan Srebro. Does invariant risk minimization capture invariance? In Arindam Banerjee and Kenji Fukumizu, editors, *Proceedings of The 24th International Conference on Artificial Intelligence and Statistics*, volume 130 of *Proceedings of Machine Learning Research*, pages 4069–4077. PMLR, 13–15 Apr 2021. URL <https://proceedings.mlr.press/v130/kamath21a.html>.
- Divyansh Kaushik, Eduard Hovy, and Zachary C. Lipton. Explaining the efficacy of counterfactually augmented data. *arXiv preprint arXiv:2010.02114*, 2020. URL <https://arxiv.org/abs/2010.02114>.
- Pang Wei Koh and Percy Liang. Understanding black-box predictions via influence functions. In *Proceedings of ICML*, 2017. URL <https://proceedings.mlr.press/v70/koh17a/koh17a.pdf>.
- Zhe Li, Wei Zhao, Yige Li, and Jun Sun. Do influence functions work on large language models? *arXiv preprint arXiv:2409.19998*, 2024.
- Hunter Lightman, Vineet Kosaraju, Yuri Burda, Harrison Edwards, Bowen Baker, Teddy Lee, Jan Leike, John Schulman, Ilya Sutskever, and Karl Cobbe. Let’s verify step by step. In *The Twelfth International Conference on Learning Representations*, 2023.

- Stephanie Lin, Jacob Hilton, and Owain Evans. Truthfulqa: Measuring how models mimic human falsehoods. *arXiv preprint arXiv:2109.07958*, 2021.
- Haotian Liu et al. Llms as narcissistic evaluators: When ego inflates evaluation scores. *arXiv preprint arXiv:2311.01964*, 2023.
- lucasmccabe. Logiqa. Hugging Face dataset, 2021. URL <https://huggingface.co/datasets/lucasmccabe/logiqa>.
- Dung Nguyen Manh, Thang Phan Chau, Nam Le Hai, Thong T Doan, Nam V Nguyen, Quang Pham, and Nghi DQ Bui. Codemmlu: A multi-task benchmark for assessing code understanding capabilities of codellms. *CoRR*, 2024.
- James Martens. Deep learning via hessian-free optimization. In *Proceedings of ICML*, pages 735–742, 2010. URL https://www.cs.toronto.edu/~jmartens/docs/Deep_HessianFree.pdf.
- Meta AI. Llama-3.2-3b-instruct — model card. <https://huggingface.co/meta-llama/Llama-3.2-3B-Instruct>, 2024a. Accessed 2025-09-09.
- Meta AI. Meta-llama-3-8b-instruct — model card. <https://huggingface.co/meta-llama/Meta-Llama-3-8B-Instruct>, 2024b. Accessed 2025-09-09.
- Paulius Micikevicius, Sharan Narang, Jonah Alben, Gregory Diamos, Erich Elsen, David Garcia, Boris Ginsburg, Michael Houston, Oleksii Kuchaiev, Ganesh Venkatesh, and Hao Wu. Mixed precision training. In *International Conference on Learning Representations (ICLR)*, 2018. URL <https://arxiv.org/abs/1710.03740>.
- Microsoft. Phi-3.5-mini-instruct — model card. <https://huggingface.co/microsoft/Phi-3.5-mini-instruct>, 2025. Accessed 2025-09-09.
- NVIDIA Corporation. Nvidia a100 tensor core gpu architecture. Whitepaper, 2020. URL <https://images.nvidia.com/aem-dam/en-zz/Solutions/data-center/nvidia-ampere-architecture-whitepaper.pdf>.
- Miruna Oprescu, Vasilis Syrgkanis, and Zhiwei Steven Wu. Orthogonal random forest for causal inference. In *International Conference on Machine Learning*, pages 4932–4941. PMLR, 2019.
- Long Ouyang, Jeff Wu, Xu Jiang, Diogo Almeida, Carroll L. Wainwright, Pamela Mishkin, Chong Zhang, and et al. Training language models to follow instructions with human feedback. In *Advances in Neural Information Processing Systems (NeurIPS)*, 2022.
- Long Pan et al. Spontaneous reward hacking in iterative self-refinement. *arXiv preprint arXiv:2307.04549*, 2023.
- Long Pan et al. Feedback loops with language models drive in-context reward hacking. *arXiv preprint arXiv:2402.06627*, 2024.
- Judea Pearl. Direct and indirect effects. In *Proceedings of UAI*, 2001. URL https://ftp.cs.ucla.edu/pub/stat_ser/r273-jsm05.pdf.
- Judea Pearl. *Causality: Models, Reasoning, and Inference*. Cambridge University Press, 2 edition, 2009.
- Barak A. Pearlmutter. Fast exact multiplication by the hessian. *Neural Computation*, 6(1):147–160, 1994. URL <https://direct.mit.edu/neco/article/6/1/147/5766/Fast-Exact-Multiplication-by-the-Hessian>.

- Qwen Team. Qwen3-1.7b — model card. <https://huggingface.co/Qwen/Qwen3-1.7B>, 2025a. Accessed 2025-09-09.
- Qwen Team. Qwen3-4b-thinking-2507 — model card. <https://huggingface.co/Qwen/Qwen3-4B-Thinking-2507>, 2025b. Accessed 2025-09-09.
- Rafael Rafailov, Yaswanth Chittepu, Ryan Park, Harshit Sushil Sikchi, Joey Hejna, Brad Knox, Chelsea Finn, and Scott Niekum. Scaling laws for reward model overoptimization in direct alignment algorithms. *Advances in Neural Information Processing Systems*, 37:126207–126242, 2024.
- Shauli Ravfogel, Yanai Elazar, Hila Gonen, Michael Twiton, and Yoav Goldberg. Null it out: Guarding protected attributes by iterative nullspace projection. *arXiv preprint arXiv:2004.07667*, 2020.
- Diederik M Roijers, Peter Vamplew, Shimon Whiteson, and Richard Dazeley. A survey of multi-objective sequential decision-making. *Journal of Artificial Intelligence Research*, 48:67–113, 2013.
- Elan Rosenfeld, Pradeep Ravikumar, and Andrej Risteski. The risks of invariant risk minimization. *arXiv preprint arXiv:2010.05761*, 2020.
- Andrew Slavin Ross, Michael C. Hughes, and Finale Doshi-Velez. Right for the right reasons: Training differentiable models by constraining their explanations. In *International Joint Conference on Artificial Intelligence (IJCAI)*, 2017.
- John Schulman, Sergey Levine, Pieter Abbeel, Michael Jordan, and Philipp Moritz. Trust region policy optimization. In *International conference on machine learning*, pages 1889–1897. PMLR, 2015.
- John Schulman, Filip Wolski, Prafulla Dhariwal, Alec Radford, and Oleg Klimov. Proximal policy optimization algorithms. *arXiv preprint arXiv:1707.06347*, 2017.
- Zhen Shao et al. Deepseekmath: Pushing the limits of mathematical reasoning in open language models. *arXiv preprint arXiv:2402.03300*, 2024. Introduces GRPO.
- Guangming Sheng, Chi Zhang, Zilingfeng Ye, Xibin Wu, Wang Zhang, Ru Zhang, Yanghua Peng, Haibin Lin, and Chuan Wu. Hybridflow: A flexible and efficient rlhf framework. *arXiv preprint arXiv: 2409.19256*, 2024.
- Ivaxi Sheth, Bahare Fatemi, and Mario Fritz. Causalgraph2llm: Evaluating llms for causal queries. In *Findings of ACL: NAACL 2025*, 2025.
- Rahul Shrama et al. Towards understanding sycophancy in language models. *arXiv preprint arXiv:2310.13548*, 2023.
- Shang Hong Sim, Tej Deep Pala, Vernon Toh, Hai Leong Chieu, Amir Zadeh, Chuan Li, Navonil Majumder, and Soujanya Poria. Lessons from training grounded llms with verifiable rewards. *arXiv preprint arXiv:2506.15522*, 2025.
- Nisan Stiennon, Long Ouyang, Jeffrey Wu, Daniel M. Ziegler, Ryan Lowe, and et al. Learning to summarize with human feedback. In *Advances in Neural Information Processing Systems (NeurIPS)*, 2020.
- Harsha Tanneru et al. On the hardness of verifying chain-of-thought faithfulness. *arXiv preprint arXiv:2411.04047*, 2024.
- Tyler J. VanderWeele. Controlled direct and mediated effects: Definition, identification and bounds. *Scandinavian Journal of Statistics*, 38(3):551–563, 2011. doi: 10.1111/j.1467-9469.2010.00722.x. URL <https://pmc.ncbi.nlm.nih.gov/articles/PMC4193506/>.

- Roman Vershynin. *High-dimensional probability: An introduction with applications in data science*, volume 47. Cambridge university press, 2018.
- Boxin Wang et al. Large language models are not fair evaluators. *arXiv preprint arXiv:2310.05492*, 2023.
- Chaoqi Wang, Zhuokai Zhao, Yibo Jiang, Zhaorun Chen, Chen Zhu, Yuxin Chen, Jiayi Liu, Lizhu Zhang, Xiangjun Fan, Hao Ma, et al. Beyond reward hacking: Causal rewards for large language model alignment. *arXiv preprint arXiv:2501.09620*, 2025.
- Jason Wei, Xuezhi Wang, Dale Schuurmans, Maarten Bosma, Brian Ichter, Fei Xia, Ed H. Chi, Quoc Le, and Denny Zhou. Chain-of-thought prompting elicits reasoning in large language models. In *Advances in Neural Information Processing Systems (NeurIPS)*, 2022.
- Yilun Wen et al. Language models learn to mislead humans via rlhf. *arXiv preprint arXiv:2409.12822*, 2024.
- Joong-Ho Won, Jason Xu, and Kenneth Lange. Projection onto minkowski sums with application to constrained learning. In *International Conference on Machine Learning*, pages 3642–3651. PMLR, 2019.
- Liang Yu et al. Towards better causal reasoning in language models. In *NAACL Long Papers*, 2025.
- Wenting Yu, Meng Jiang, Peter Clark, and Ashish Sabharwal. Ifqa: Counterfactual open-domain qa. GitHub repository, 2023. URL <https://github.com/wyu97/IfQA>.
- Weizhe Yuan, Richard Yuanzhe Pang, Kyunghyun Cho, Xian Li, Sainbayar Sukhbaatar, Jing Xu, and Jason Weston. Self-rewarding language models. *arXiv preprint arXiv:2401.10020*, 2025.
- Tianyi Zhang, Varsha Kishore, Felix Wu, Kilian Q Weinberger, and Yoav Artzi. Bertscore: Evaluating text generation with bert. *arXiv preprint arXiv:1904.09675*, 2019.
- Lianmin Zheng, Wei-Lin Chiang, Ying Sheng, Siyuan Zhuang, Zhanghao Wu, Yonghao Zhuang, Zi Lin, Zhuohan Li, Dacheng Li, Eric Xing, et al. Judging llm-as-a-judge with mt-bench and chatbot arena. *Advances in neural information processing systems*, 36:46595–46623, 2023.
- Yujun Zhou, Zhenwen Liang, Haolin Liu, Wenhao Yu, Kishan Panaganti, Linfeng Song, Dian Yu, Xiangliang Zhang, Haitao Mi, and Dong Yu. Evolving language models without labels: Majority drives selection, novelty promotes variation. *arXiv preprint arXiv:2509.15194*, 2025.

A. Related Works

A.1. Reward Hacking in LLM

Reward hacking occurs when models exploit imperfections in reward functions rather than achieving the intended objective [Amodei et al., 2016, Everitt et al., 2017, Zhou et al., 2025]. In large language models, this problem emerges prominently under alignment: proxy reward models can be gamed, leading to behaviors such as generating superficially persuasive but incorrect answers Wen et al. [2024], sycophancy Shrama et al. [2023], and exploiting evaluator biases in LLM-as-judge settings Liu et al. [2023], Wang et al. [2023]. More recently, iterative refinement has revealed *in-context reward hacking*, where models adapt outputs to maximize evaluation scores rather than genuinely improving reasoning quality Pan et al. [2023, 2024]. Mitigation strategies typically involve improved supervision (e.g., rationale-level feedback Ross et al. [2017]), evaluator debiasing, or structural interventions such as counterfactual augmentation Kaushik et al. [2020] and invariance penalties Arjovsky et al. [2020]. However, these often rely on external annotations nor emphasized robustness–accuracy trade-offs. Our method introduces differentiable, counterfactual-enhanced causal signals as internal rewards, jointly optimizing accuracy and causal coherence to directly curb shortcut exploitation.

A.2. Causal Inference and Reasoning in LLMs

There have been several studies centering on causal reasoning capability in LLMs. Corr2Cause finds poor correlation-to-causation transfer by pure LLM reasoning [Jin et al., 2024], CoT often fails to be causally responsible for answers [Bao et al., 2024a], and faithful CoT remains challenging even with fine-tuning or activation edits [Tanneru et al., 2024]. Methods that *impose* causal structure are emerging (e.g., G²-Reasoner combines knowledge and goal prompts to improve causal reasoning) [Chi et al., 2025]. Mechanistic approaches intervene directly in internal representations—editing factual circuits and testing hypotheses via causal/activation patching—to probe and modify pathways [Heimersheim et al., 2024]. There also several studies utilizing SCM [Yu et al., 2025] and causal graph [Sheth et al., 2025] for better reasoning. Yet most studies are *post-hoc*. We build on this direction by using interventional, pathway-aware signals during post-training, and by explicitly aggregating them with task rewards to control the accuracy–causal-coherence trade-off.

B. Theoretical Guarantees

Setup. Let π, π_{old} be stationary policies, $\gamma \in (0, 1)$ the discount factor, and d^π the normalized discounted state distribution. Fix the baseline policy π_{old} and let $A(s, a) = A_{\pi_{\text{old}}}(s, a)$ be its advantage under the CE-PO reward r_{CE} (the Minkowski combiner of all channels). For each state s , denote by $\mathcal{N}_s \subset \mathbb{R}^{|\mathcal{A}|}$ the subspace spanned by *nuisance directions* (e.g., verbosity/length) estimated via counterfactual perturbations, and let P_s be the Euclidean orthogonal projector onto \mathcal{N}_s . Write the action simplex $\Delta^{|\mathcal{A}|} = \{p \in \mathbb{R}^{|\mathcal{A}|} : p \geq 0, \mathbf{1}^\top p = 1\}$ with tangent space $\mathcal{T}_s = \{v \in \mathbb{R}^{|\mathcal{A}|} : \mathbf{1}^\top v = 0\}$. Define the *orthogonalized advantage*

$$A_\perp(s, \cdot) := (I - P_s) A(s, \cdot), \quad \varepsilon_\perp := \max_s \|A_\perp(s, \cdot)\|_\infty.$$

and let

$$\alpha := \max_s D_{\text{TV}}(\pi(\cdot|s), \pi_{\text{old}}(\cdot|s)) = \frac{1}{2} \max_s \|\pi(\cdot|s) - \pi_{\text{old}}(\cdot|s)\|_1.$$

The TRPO-style surrogate is

$$L_{\pi_{\text{old}}}^{\text{CE}}(\pi) = \eta_{\text{CE}}(\pi_{\text{old}}) + \frac{1}{1 - \gamma} \mathbb{E}_{s \sim d^{\pi_{\text{old}}}} [\langle A(s, \cdot), \pi(\cdot|s) - \pi_{\text{old}}(\cdot|s) \rangle],$$

noting that $\langle A(s, \cdot), \pi_{\text{old}}(\cdot|s) \rangle = 0$ for all s .

Assumptions and Propositions

P0 (Fixed reward at π_{old}) All CE components used to construct r_{CE} (Jacobians, counterfactual subspaces \mathcal{N}_s , projectors P_s , and channel scores) are computed at π_{old} and held fixed while evaluating $\eta_{\text{CE}}(\pi)$ over one update step.

A0 (Residualization on the action-simplex tangent) By construction of r_{CE} via counterfactual projection, the CE advantage is locally invariant along nuisance directions at π_{old} :

$$\langle A(s, \cdot), v \rangle = 0 \quad \text{for all } v \in \mathcal{N}_s \cap \mathcal{T}_s.$$

Equivalently, $P_s A(s, \cdot) = 0$ and hence $A(s, \cdot) = A_{\perp}(s, \cdot) \in \mathcal{N}_s^{\perp}$.

A1 (Well-posedness & bounded rewards) Base rewards and channel scores are in $[0, 1]$ and CE weights sum to one, so $r_{\text{CE}} \in [0, 1]$. The MDP is standard (finite or σ -finite), ensuring existence of $V^{\pi}, Q^{\pi}, A_{\pi}$.

Theorem 1 (Orthogonalized TRPO Lower Bound for CE-PO). For any π , with $\alpha = \max_s D_{\text{TV}}(\pi(\cdot|s), \pi_{\text{old}}(\cdot|s))$, the CE-PO performance satisfies

$$\eta_{\text{CE}}(\pi) \geq L_{\pi_{\text{old}}}^{\text{CE}}(\pi) - \frac{4\gamma}{(1-\gamma)^2} \varepsilon_{\perp} \alpha^2. \quad (8)$$

Proof. Step 1: Performance-difference decomposition. The performance-difference lemma gives

$$\eta_{\text{CE}}(\pi) - \eta_{\text{CE}}(\pi_{\text{old}}) = \frac{1}{1-\gamma} \mathbb{E}_{s \sim d^{\pi}} [\langle A(s, \cdot), \pi(\cdot|s) \rangle].$$

Add and subtract the surrogate:

$$\eta_{\text{CE}}(\pi) = L_{\pi_{\text{old}}}^{\text{CE}}(\pi) + \frac{1}{1-\gamma} \mathbb{E}_s \left[(d^{\pi} - d^{\pi_{\text{old}}})(s) \langle A(s, \cdot), \pi(\cdot|s) \rangle \right] =: L_{\pi_{\text{old}}}^{\text{CE}}(\pi) - \frac{1}{1-\gamma} T,$$

so it suffices to bound $|T|$.

Step 2: Bounding the occupancy shift. By a standard coupling argument, $\|d^{\pi} - d^{\pi_{\text{old}}}\|_1 \leq \frac{2\gamma}{1-\gamma} \alpha$. Thus

$$|T| \leq \left(\max_s |\langle A(s, \cdot), \pi(\cdot|s) \rangle| \right) \|d^{\pi} - d^{\pi_{\text{old}}}\|_1 \leq \frac{2\gamma}{1-\gamma} \alpha \max_s |\langle A(s, \cdot), \pi(\cdot|s) \rangle|.$$

Step 3: Using CE-PO orthogonalization (A1). For each s , by A1 we have $A(s, \cdot) = A_{\perp}(s, \cdot) \in \mathcal{N}_s^{\perp}$, and $\langle A(s, \cdot), \pi_{\text{old}}(\cdot|s) \rangle = 0$ (definition of advantage). Hence

$$\langle A(s, \cdot), \pi(\cdot|s) \rangle = \langle A_{\perp}(s, \cdot), \pi(\cdot|s) - \pi_{\text{old}}(\cdot|s) \rangle \leq \|A_{\perp}(s, \cdot)\|_{\infty} \|\pi(\cdot|s) - \pi_{\text{old}}(\cdot|s)\|_1 \leq 2\varepsilon_{\perp} \alpha.$$

Taking the supremum over s yields $\max_s |\langle A(s, \cdot), \pi(\cdot|s) \rangle| \leq 2\varepsilon_{\perp} \alpha$, and therefore

$$|T| \leq \frac{2\gamma}{1-\gamma} \alpha (2\varepsilon_{\perp} \alpha) = \frac{4\gamma}{1-\gamma} \varepsilon_{\perp} \alpha^2.$$

Step 4: Final bound. Plugging into Step 1,

$$\eta_{\text{CE}}(\pi) \geq L_{\pi_{\text{old}}}^{\text{CE}}(\pi) - \frac{4\gamma}{(1-\gamma)^2} \varepsilon_{\perp} \alpha^2,$$

which is inequality (8). \square

Properties. (*Tightening via nuisance removal, ℓ_2 statement*). Let $\varepsilon_{\text{base}}^{(2)} := \max_s \|A_{\text{base}}(s, \cdot)\|_2$ be the corresponding constant under a non-residualized baseline reward, and define $\varepsilon_{\perp}^{(2)} := \max_s \|A_{\perp}(s, \cdot)\|_2$. If there exists $\rho \in (0, 1]$ such that $\|P_s A_{\text{base}}(s, \cdot)\|_2 \geq \rho \|A_{\text{base}}(s, \cdot)\|_2$ for all s (*nontrivial nuisance energy*), then by Pythagoras for orthogonal projectors,

$$\varepsilon_{\perp}^{(2)} \leq \sqrt{1 - \rho^2} \varepsilon_{\text{base}}^{(2)}.$$

Since $\|\cdot\|_{\infty} \leq \|\cdot\|_2$, we also have $\varepsilon_{\perp} \leq \varepsilon_{\perp}^{(2)}$, yielding a strictly smaller penalty constant in the ℓ_2 analogue of equation 8 (and a looser but still improved constant in ℓ_{∞} up to norm equivalence).

(*Null penalty for hacking-only updates*). If for some s the per-state policy change lies entirely in \mathcal{N}_s , i.e., $\pi(\cdot|s) - \pi_{\text{old}}(\cdot|s) \in \mathcal{N}_s$, then $(I - P_s)(\pi - \pi_{\text{old}}) = 0$ and hence $\langle A_{\perp}(s, \cdot), \pi(\cdot|s) - \pi_{\text{old}}(\cdot|s) \rangle = 0$, so that state contributes nothing to the penalty term in equation 8.

KL-based corollaries. By Pinsker’s inequality $D_{\text{TV}}(p, q) \leq \sqrt{\frac{1}{2} \text{KL}(p||q)}$, if $\delta := \max_s \text{KL}(\pi_{\text{old}}(\cdot|s)||\pi(\cdot|s))$, then

$$\eta_{\text{CE}}(\pi) \geq L_{\pi_{\text{old}}}^{\text{CE}}(\pi) - \frac{2\gamma}{(1 - \gamma)^2} \varepsilon_{\perp} \delta. \quad (9)$$

If only an *expected* per-state KL is enforced, $\mathbb{E}_{s \sim d^{\pi_{\text{old}}}} [\text{KL}(\pi_{\text{old}}||\pi)] \leq \bar{\delta}$, then equation 9 holds with $\delta = C \bar{\delta}$ for a method-dependent constant $C \geq 1$ (e.g., via ratio clipping or per-state caps used in TRPO/PPO).

From counterfactual Jacobians to action-space nuisance. Let \mathcal{U}_s be a finite set of representation-space directions obtained from counterfactual Jacobians (e.g., top singular vectors of counterfactual J_{AB} blocks), and let g_s be a smooth channel-score functional (e.g., spectral energy share). Write $G_s := \nabla_{\pi(\cdot|s)} g_s$ for its Jacobian with respect to action probabilities. Define

$$\mathcal{N}_s := \text{span}\{G_s^{\top} u : u \in \mathcal{U}_s\} \cap \mathcal{T}_s.$$

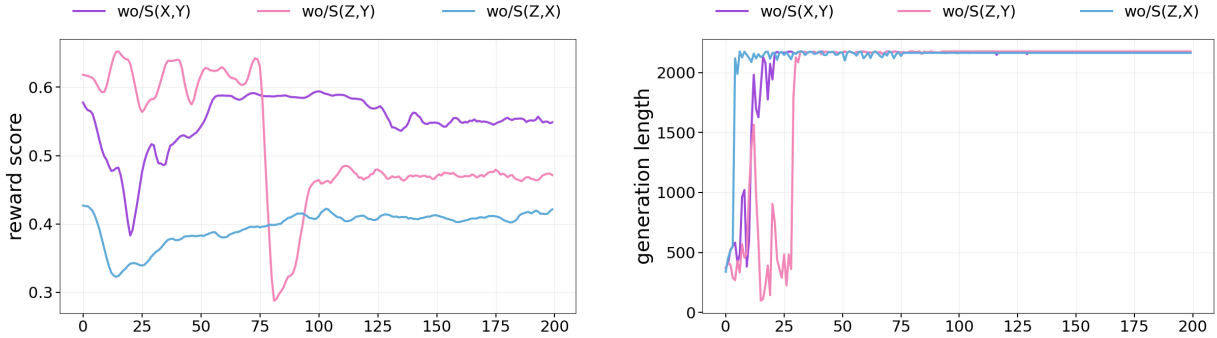
If each channel score is *residualized* by projecting J_{AB} onto \mathcal{U}_s^{\perp} , then, at π_{old} , the resulting CE reward satisfies $\langle \nabla_{\pi} r_{\text{CE}}(s, \cdot), v \rangle = 0$ for all $v \in \mathcal{N}_s \cap \mathcal{T}_s$, implying $P_s A(s, \cdot) = 0$ (Assumption A0).

C. Additional Techniques

Jacobian causal score is time and space-efficient in LLMs. We design the Jacobian-based causal reward to be *practical at scale*: it reuses forward activations, avoids any explicit Jacobian/Hessian materialization, and replaces costly subspace operations with a constant-time projection. Concretely, we rely on three tricks. (i) *Local Jacobian via vJP (vector–Jacobian Projection)*. Sensitivities are computed with one forward and two backward passes using vector–Jacobian products (reverse-mode autodiff), i.e., for a test direction U we use $\text{vJP}(s_B, E(A); U) = \langle J_{AB}, U \rangle_F = J_{AB}^{\top} \text{vec}(U)$ and the scalar sensitivity $\|J_{AB}^{\top} \text{vec}(U)\|_2$; so no dense $J \in \mathbb{R}^{T d \times T d}$ (or Hessian) is ever formed; working memory stays at $\mathcal{O}(T d)$ for token embeddings [Baydin et al., 2018, Pearlmutter, 1994]. (ii) *Residual projection*. The counterfactual direction is removed with a single inner product: if g is the local Jacobian direction and \hat{c} the (reshuffled) counterfactual direction, we use $r = g - (g^{\top} \hat{c}) \hat{c}$, avoiding SVD/subspace construction and extra buffers [Golub and Van Loan, 2013]. (iii) *Mixed precision*. Forward/backward in FP16/bfloat16 with dynamic loss scaling provides wall-clock gains while roughly halving activation memory, without changing the algorithmic interface [Micikevicius et al., 2018, NVIDIA Corporation, 2020].

Throughput and footprint. On a single modern GPU (e.g., A100 80 GB) and Llama-3-8B-Instruct, our implementation returns a reward in ≈ 2 s, with negligible persistent memory beyond base activations and the $\mathcal{O}(Td)$ embedding cache.

D. Additional Plots



(a) Reward score

(b) Mean length

Figure 11: This figure supplements the ablation analysis and demonstrates that omitting a single Jacobian term induces reward degradation accompanied by length inflation.

Question. Context: For husbands that don't set the alarm, the probability of ringing alarm is 90%. For husbands that set the alarm, the probability of ringing alarm is 25%. Question: For husbands that set the alarm, would it be less likely to see ringing alarm if the husband had not set the alarm?

Ground Truth: No

Method	Prediction (Reasoning)
BERTScore	Predicts "Yes"; relies on surface overlap (...compares 25% vs 90% directly but ignores that the subject of "less likely" is "not set").
Jacobian Only	Predicts "Yes"; observes $25\% < 90\%$ but misplaces the subject, treating "set" as the focus of "less likely" instead of "not set".
CE-GRPO	Predicts "No"; correctly checks whether $90\% < 25\%$ (false) and concludes "not set" actually makes ringing more likely, matching ground truth.

Takeaways.

- **Jacobian Only** tends to *template-follow*: latches onto "less likely \Rightarrow smaller %" and ignores subject/polarity flips, causing causal misread.
- **BERTScore** measures overlap, not causal/conditional structure; it cannot reason about which condition the "less likely" modifies.

Figure 12: Comparison of methods on the alarm-setting counterfactual example on Qwen-3-4B-Thinking.

E. Broader Impact

The proposed CE-PO framework has the potential to substantially improve the reliability and trustworthiness of large language models. By explicitly rewarding causal coherence in addition to task accuracy, the method reduces the tendency of models to exploit superficial cues or engage in reward hacking, which can lead to misleading or unfaithful reasoning. In practice, this enables LLMs to

generate explanations and rationales that are not only correct in outcome but also grounded in meaningful reasoning processes—an essential property for high-stakes domains such as law, science, medicine, and education.

Beyond improving alignment, CE-PO can serve as a general methodology for building AI systems that are “right for the right reasons,” supporting transparency, auditability, and robustness under distribution shifts. This contributes to safer deployment of generative models in real-world decision-making pipelines. At the same time, emphasizing causal regularization may help mitigate harmful biases that arise when models rely on spurious correlations, thereby supporting more equitable AI systems.

F. Prompt Templates

We presented the prompt template for clear Z , X , Y separation in Figure 13 and detailed instruction for LLM-as-Judge in Figure 14.

Prompt Instructions (Final Answer Tagging)

```
"Solve the question and generate in assigned format."
"Wrap your final answer between <finalanswer> </finalanswer> tags. "
"It's mandatory and required to not include anything after </finalanswer>
tag. Don't let your generation process to redundant and lengthy."
"Be very clear in your explanation, and ensure the final answer is presented
separately."
"Example of output: We analyze A, solve B and answer is C. So final answer
is <finalanswer> C is correct </finalanswer>"
```

Figure 13: Verbatim instructions for final-answer tagging.

Table 3: Welch’s t -tests comparing $S(A, B)$ distributions between Incorrect and Correct groups.

Metric	t	p -value
$S(Z, X)$	3.55	0.0005
$S(X, Y)$	3.23	0.0014
$S(Z, Y)$	3.15	0.0018

G. Dataset Features

H. The Use of Large Language Models (LLMs)

LLMs are the primary subject of our reinforcement learning (RL) experiments: we fine-tune pretrained models under CE-PO and baseline objectives to study stability, reward hacking, and causal alignment. Separately, we use LLMs as utilities for controlled text transformations—rephrasing, grammar correction, and during writing phase.

Prompt Template (Strict Judge)**Task**

Decide if the final answer **matches** the ground truth.

Rules (both must hold)

- 1) **Final-answer equivalence**: extract the last explicit final answer and compare it to the ground truth *after trimming whitespace and ignoring case*.
- 2) **Reasoning validity** : Validity ($Z \rightarrow X \rightarrow Y$): Z must substantiate X, and Z,X must substantiate Y. Accept only reasoning that is logically sound, evidence-backed, and contradiction-free; apply near-adversarial scrutiny—any gaps, guesses, or inconsistencies $\rightarrow 0$.

Question Z

{question}

Ground Truth Answer

{correct_answer}

Provided Reasoning X+Y

{reasoning_process}

Output (plain-text JSON, no code fences)

```
{
  "judge_explanation": "<brief explanation>",
  "result": "<Yes or No>"
}
```

Figure 14: Prompt template for strict binary judgment requiring answer equivalence and valid reasoning.

Table 4: Training Dataset

Dataset	Question	Answer
BBEHCausal	Question: Alice (AF) and Bob (BF) each fire a bullet at a window, simultaneously striking the window. The window only shatters (WS) if it is hit by two bullets. Is Alice firing the bullet a sufficient cause for the window shattering? Reply based on the answer a logician would give.	No
CasHOLD	Context: limitations was equitably tolled fails because he did not raise this argument before the district court. See Hinton v. Pac. Enters., 5 F.3d 391, 395 (9th Cir.1993) (HOLDING). Grace’s remaining contentions lack merit. Select the correct holding (1 to 4): "holding that the burden to allege facts sufficient to establish jurisdiction resides with plaintiff", "holding that the plaintiff bears the burden when relying on the discovery rule", "recognizing the validity of the doctrine but holding no equitable tolling on the facts presented", "holding that plaintiff bears the burden to timely allege facts supporting equitable tolling", "holding that the burden is on the plaintiff to allege facts sufficient to establish jurisdiction"	3: "holding that plaintiff bears the burden to timely allege facts supporting equitable tolling"
MATHHARD	There are thirty-five red, yellow, orange, and white marbles in a bag. If half the number of red marbles equals two less than the number of yellow marbles, equals a third the number of orange marbles, and equals a third of three more than the number of white marbles, how many red marbles are there?	8
IfQA	If Caroline Flack’s mother had felt the name suited her, what would have been Caroline’s name?	Caroline

Table 5: Testing Dataset

Dataset	Question	Answer
BBEHMATH	<p>Consider the operations $a \ [] \ b =$</p> $\begin{cases} (a - b), & a + b > 0 \\ -a - -b, & \text{otherwise} \end{cases}, \quad a \ ; \ b =$ $\begin{cases} (b - a) * b, & a - b < 2 \\ (a - b) * a, & \text{otherwise} \end{cases}, \quad a \ ! \ b =$ $\begin{cases} (2 \ [] \ b) * a, & a > b \\ b, & \text{otherwise} \end{cases}, \quad \text{and } a \ @ \ b =$ $\begin{cases} (a \ ! \ b), & a - b > 0 \\ a * b, & \text{otherwise} \end{cases}; \quad \text{define } A =$ $(((-5; -7) + (2 @ -4)) \ [] \ ((-9 \ [] \ -2) \ ! \ (6 \cdot 1))) \ []$ $(((7 - 6) \ [] \ (6 + -6)) \cdot ((-2 \ [] \ 9); (-1 - 5))),$ $B = (((9; 7) \ [] \ (6 \cdot 7)) \ [] \ ((2! - 2) + (3 \ [] \ -6)));$ $(((1 - 8) + (-5 @ -5)); ((-4 - 10); (-3 @ 6))),$ <p>and $C = (((-10! - 1) \ ! \ (-5 + -6)) @ ((-8 + 5) \cdot (-10 + 10))); (((-3 - 3); (2 \ [] \ -5)) - ((2 \cdot 9) - (-8 \ [] \ 2)));$ compute $A + B - C$ (answer as a number).</p>	-10038
CLadder	<p>Context: For husbands that don't set the alarm, the probability of ringing alarm is 42%. For husbands that set the alarm, the probability of ringing alarm is 51%. Question: For husbands that set the alarm, would it be less likely to see ringing alarm if the husband had not set the alarm?</p>	yes
LegalBench	<p>Context: Overall, the percentages and correlation coefficients in nine of the ten endogenous are sufficient for purposes of the second Gingles precondition. See 478 U.S. at 56. Plaintiffs have shown minority political cohesiveness in these [**105] appellate-judgeship elections. Nonetheless, the stark statistic remains that, in Alabama's history, only two African Americans have been elected to statewide office for a total of [**186] three general elections and three primary elections. At the statewide level, this factor weighs in favor of Plaintiffs. Question: Based on the excerpt above, did the judge's legal reasoning rely on statistical evidence (e.g., regression analysis) when determining whether there was a causal link? Answer Yes or No</p>	Yes
LogiQA	<p>Some purple clay pots are alive. Therefore, some living things have good or bad quality. Question: Which of the following judgments, if true, would best strengthen the argument? Options: ['The quality of purple clay teapots is different from good to bad.', 'Some purple clay pots are inanimate.', 'There is no difference in the quality of purple clay teapots.', 'Some living things are not purple clay pots.']</p>	0, The quality of purple clay teapots is different from good to bad.